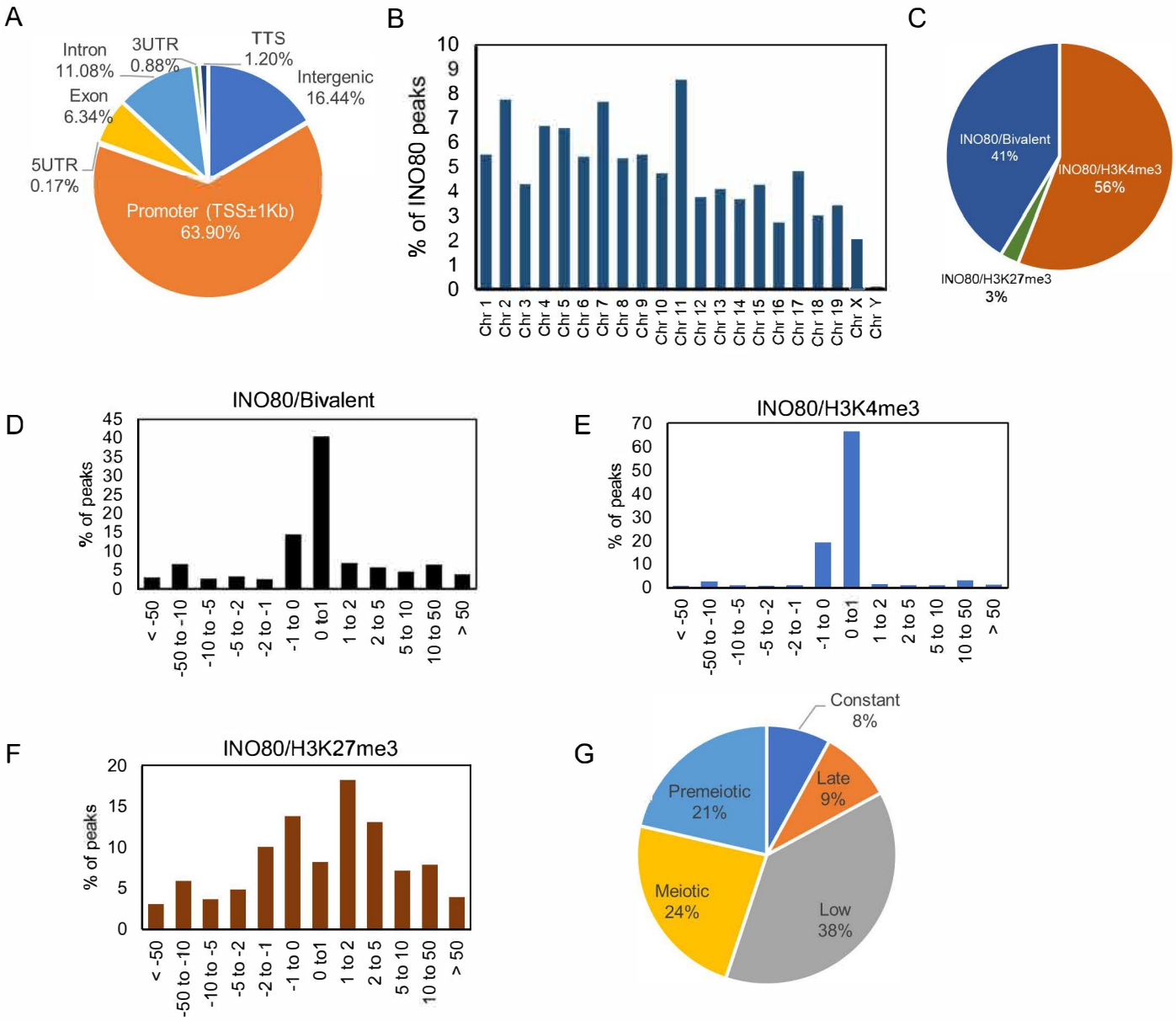

Fig. S1. Features of genome-wide INO80 localization. (A) Relative distribution of INO80 binding sites among different genomic annotations. (B) Distribution of INO80 binding sites among all the autosomes and sex chromosomes. (C) Relative occurrence of INO80 binding sites that either co-localize with H3K4me3 or H3K27me3, or with both H3K4me3 and H3K27me3 among promoters. (D-F) Distance of INO80 peaks that co-localize with either H3K4me3 or H3K27me3, or with both H3K4me3 and H3K27me3. (G) Percentage of genes from the five temporal gene expression cohorts that interact with INO80 at their promoter.

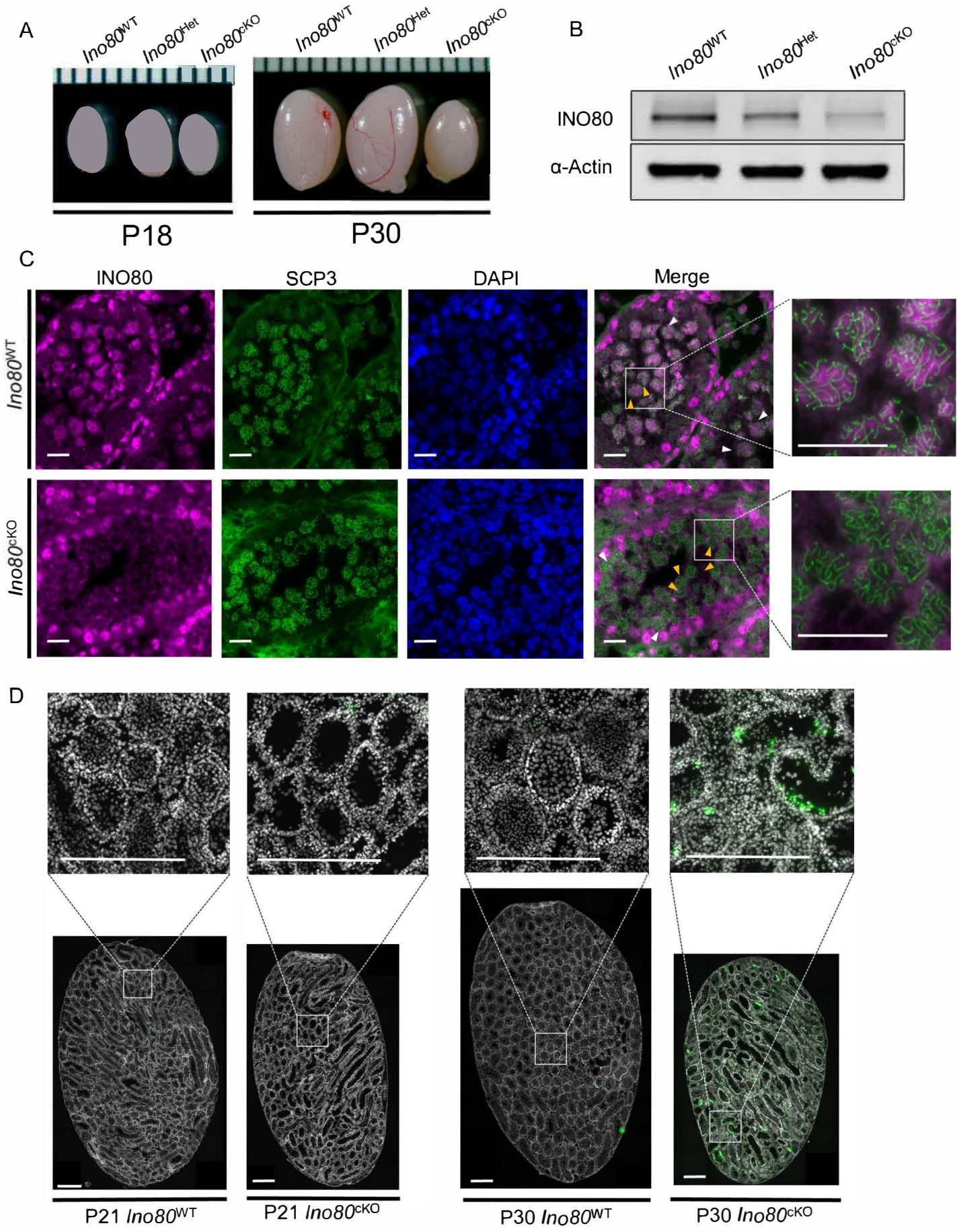
A
Ino80WT
Ino80Het
Ino80cKO
Ino80WT
Ino80Het
Ino80cKO
P18
P30
B
Ino80WT
Ino80Het
Ino80cKO
INO80
α-Actin
C
INO80
SCP3
DAPI
Merge
Ino80WT
Ino80cKO
D
P21 Ino80WT
P21 Ino80cKO
P30 Ino80WT
P30 Ino80cKO

Fig. S2. *Ino80* deletion in the prepubertal testis. (A) Image exhibiting the size of whole testis dissected from either *Ino80*^{WT}, *Ino80*^{Het} and *Ino80*^{cKO} mice on P18 and P30. (B) Immunoblot showing INO80 protein expression levels in *Ino80*^{WT}, *Ino80*^{Het} and *Ino80*^{cKO} testes in 3-week-old mice. (C) Immunofluorescence analysis showing INO80 expression in either *Ino80*^{WT} or *Ino80*^{cKO} testis sections. Magenta represents INO80, green is SYCP3, and blue is DAPI. White arrowheads represent zygotene spermatocytes and yellow arrowheads represent pachytene spermatocytes. Scale bar = 20μM. (D) TUNEL staining showing presence of apoptotic nuclei (green) in either *Ino80*^{WT} or *Ino80*^{cKO} testis sections from P21 and P30 mice, counterstained with DAPI (Grey). Scale bar = 0.5mM.

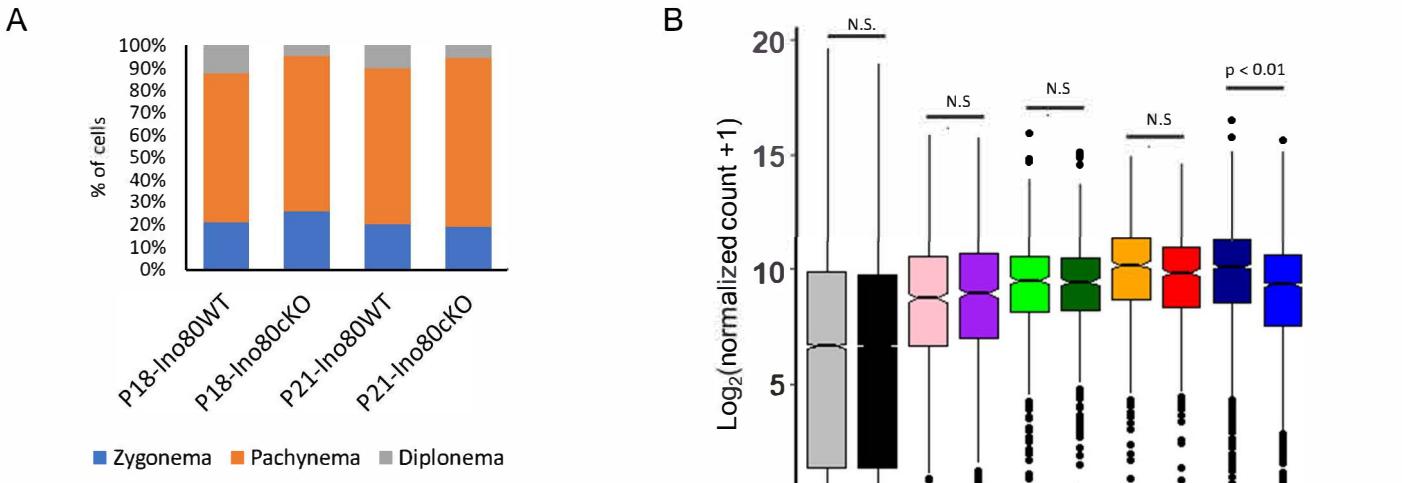

Fig. S3. Composition of spermatocyte stages in response to *Ino80* deletion. (A) Comparison of cellular composition between *Ino80*^{WT} and *Ino80*^{cKO} testis at either P18 or P21. (B) Comparison of expression from gene signatures (from Ball et al., 2016) for either spermatogonia (Spg), leptotene/zygotene spermatocytes (L-Z), early pachytene spermatocytes (EP), or late pachytene/diplotene spermatocytes (LP-D). Included are all expressed genes (All) from either *Ino80*^{WT} or *Ino80*^{cKO} spermatocytes. N.S., Non significant. *P*-value derived from one-way ANOVA with Tukey's post hoc test.

Chakraborty_Supplemental_Figure_S4

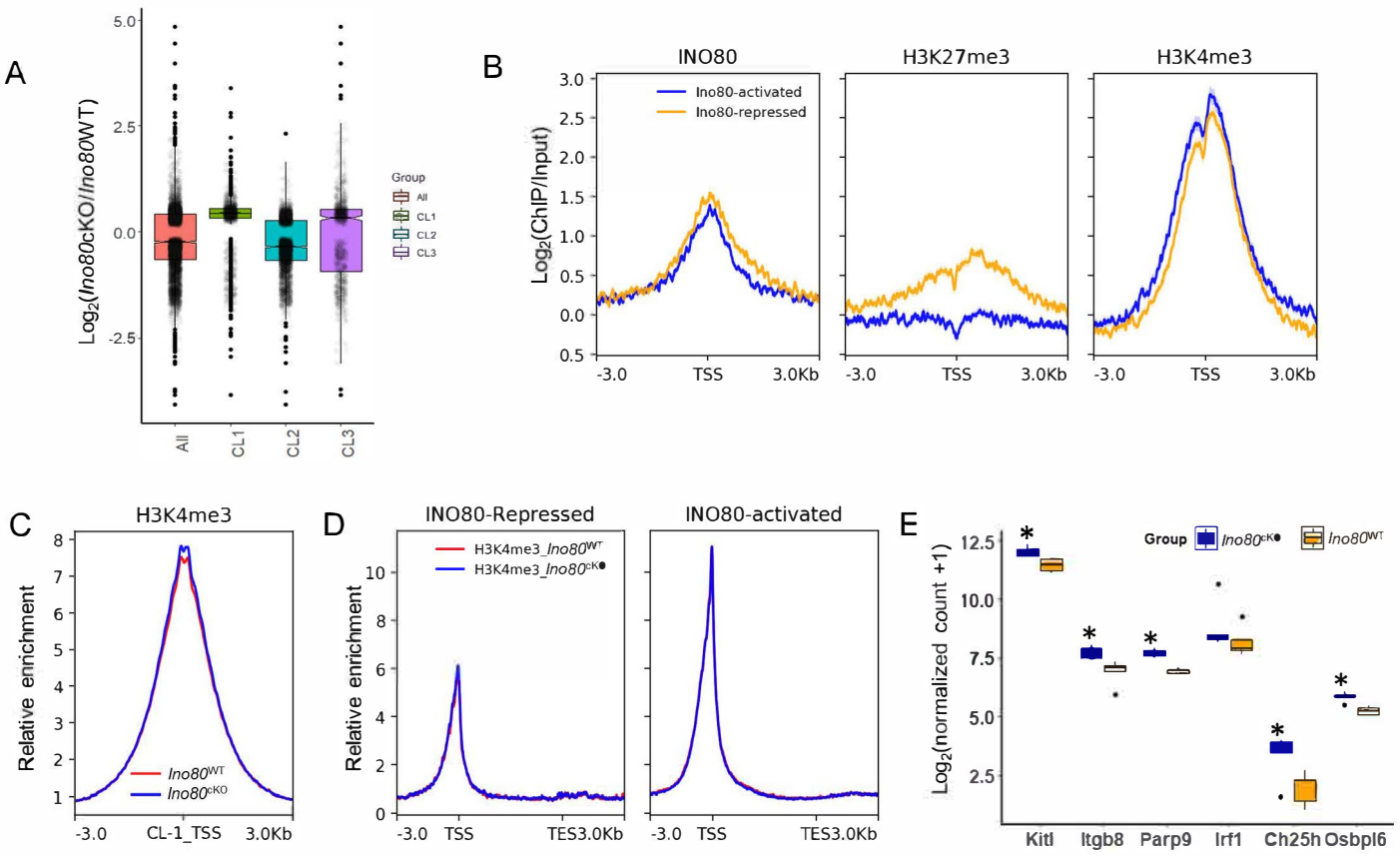

Fig. S4. Change in gene expression and histone modifications due to *Ino80* deletion. (A) Boxplot showing average changes in overall gene expression for either all expressed genes or for each subset present in gene clusters based on INO80 binding, and histone modification. Dots represent Log_2fold change of individual genes. (B) Metaplots exhibiting relative enrichment of either INO80, H3K27me3 or H3K4me3 at the TSS of all differentially regulated genes, either upregulated (INO80-repressed; yellow) or downregulated (INO80-activated; blue) in *Ino80*^{cKO} spermatocytes compared to *Ino80*^{WT}. (C) Metaplots showing relative enrichment for H3K4me3 between *Ino80*^{cKO} and *Ino80*^{WT} for CL-1. Plots are centered at the TSS. (D) Metaplot summarizing the relative enrichment of H3K4me3 at the TSS of INO80-activated and INO80-repressed genes in either *Ino80*^{WT} or *Ino80*^{cKO} spermatocytes. (E) Relative expression of representative genes in either *Ino80*^{WT} or *Ino80*^{cKO} spermatocytes from RNAseq data (*, p-adjust<0.05, n=5).

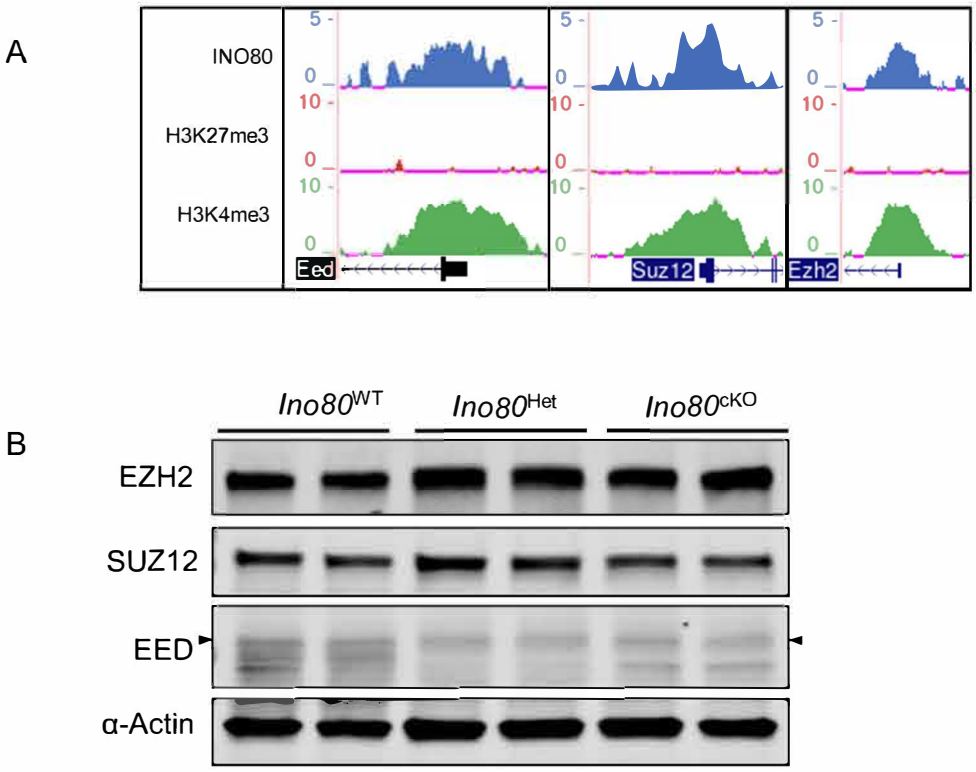

Fig. S5. Promoter activity and expression of PRC2 subunits. (A) Genomic tracks exhibiting INO80, H3K27me3 and H3K4me3 binding at PRC2 subunit genes such as SUZ12, EZH2, RBBP4 and EED. (B) Immunoblot showing the protein expression levels of EZH2, SUZ12, EED and alpha Actin in *Ino80*^{WT}, *Ino80*^{Het} and *Ino80*^{cKO} spermatocytes on P18.

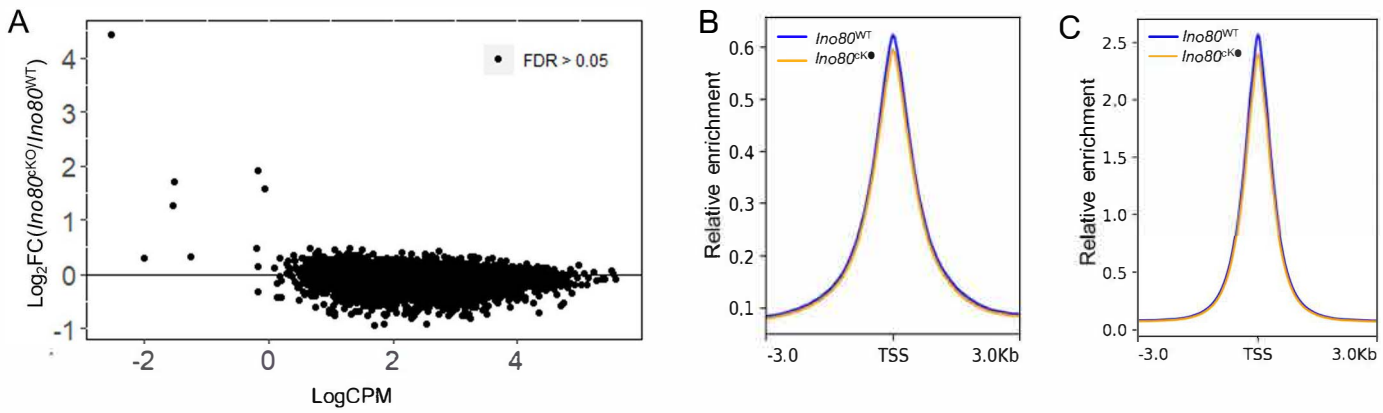

Fig. S6. Chromatin accessibility at bivalent sites. (A) Dot plot showing individual ATAC peaks at the INO80-interacting bivalent sites (CL-1). Black dots represent FDR > 0.05. FDR was derived by Benjamini-Hochberg method (n=3). (B-D) Metaplot showing changes in the average ATAC signal in either *Ino80*^{WT} or *Ino80*^{cKO} spermatocytes at CL-1 (B) and CL-2 (C).

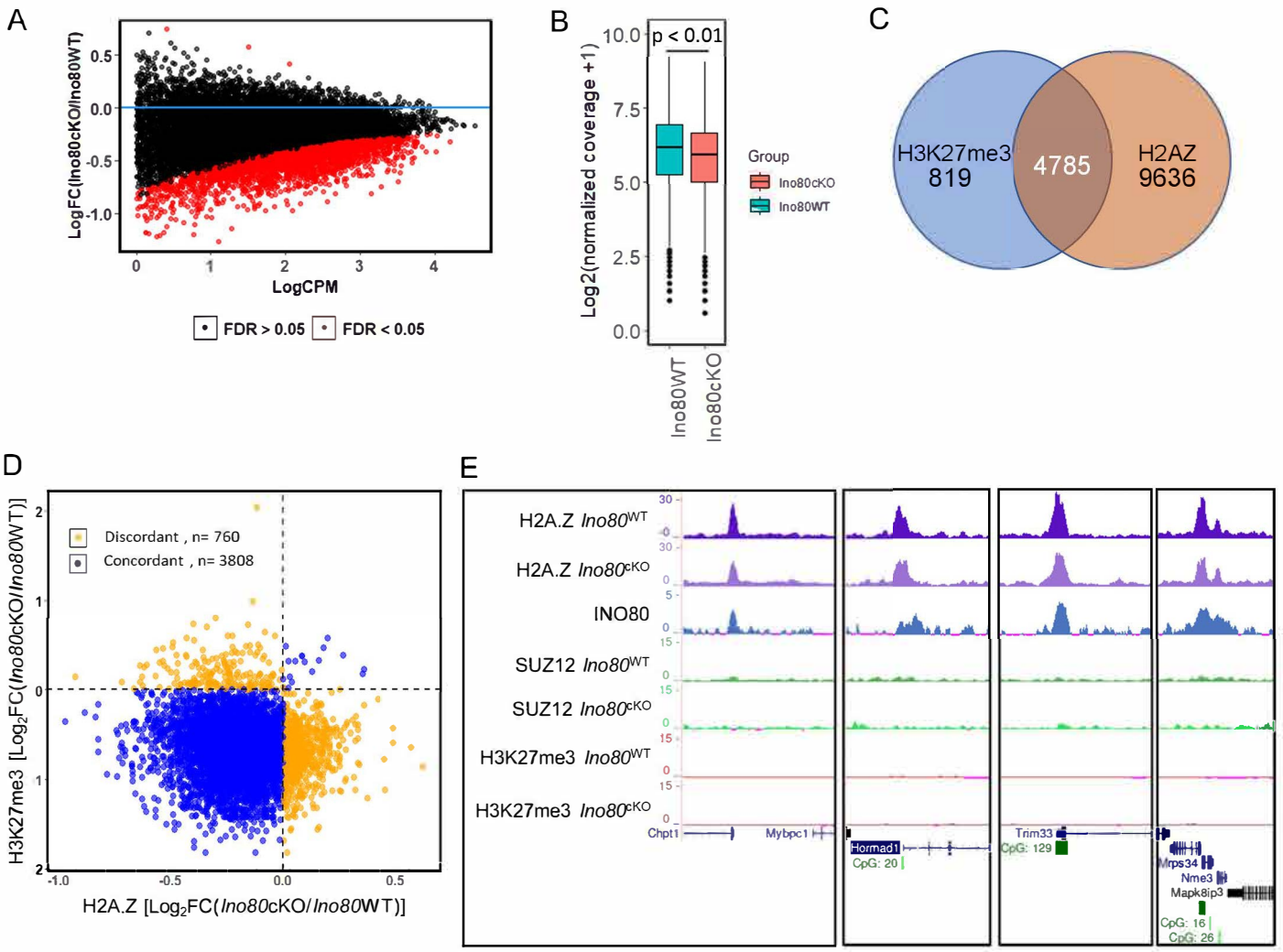

Fig. S7. Genomewide H2A.Z occupancy in response to *Ino80* deletion. (A) Dot plot showing differential analysis of H2A.Z binding at INO80 peaks. Red dots represent promoters that have significant (FDR < 0.05) changes in H2A.Z enrichment in *Ino80*^{cKO} compared to *Ino80*^{WT}. Black dots represent FDR > 0.05. FDR was derived by Benjamini-Hochberg method (n=2). (B) Comparison of normalized coverage for H2A.Z between *Ino80*^{cKO} and *Ino80*^{WT} at INO80 interacting regions. *P*<0.01, as calculated by Wilcoxon signed rank test. (C) Venn diagram illustrating the number of promoters that have either H3K27me3, or H2A.Z or both. (D) Dot plot showing either concordant or discordant changes in either H3K27me3 or H2A.Z enrichment between *Ino80*^{cKO} and *Ino80*^{WT}. (E) Genomic track showing enrichment of H2A.Z, SUZ12 and H3K27me3 and INO80 at representative genes devoid of both SUZ12 and H3K27me3.

Table S1. List of INO80 peaks from ChIP-seq on wild type P18 spermatocytes.

Click here to download Table S1

Table S2. List of differentially regulated genes upon *Ino80* deletion in P18 spermatocytes.

Click here to download Table S2

Table. S3. List of H2A.Z peaks from ChIP-seq on wild type P18 spermatocytes.

Click here to download Table S3

Table S4. Genotyping primers used in this study.

Allele	Sequence
Ino80 floxed forward	5'-GATACTTCTGCCTCCACACTTC-3'
Ino80 floxed reverse	5'-CTGGCACCTTTCCAGTCTTT-3'
Ino80 excised forward	5'-TGTGTAGCAACCTACAGCTA-3'
Ino80 excised reverse	5'-GTTGCTGTGTCTTTGCTTTG-3'
Stra8Cre forward	5'-GTGCAAGCTGAACAACAGGA-3'
Stra8Cre reverse	5'-AGGGACACAGCATTGGAGTC-3'

Table S5. Primary antibodies used in this study.

Primary antibody	Source	Amount/Dilution
Rabbit anti-INO80	Abcam (ab105451)	ChIP-seq (10µg) WB (1:2000) IF (1:700)
Rabbit anti-INO80	Novus Biologicals (NBP1-78758)	IP (10 µg)
Rabbit anti-SUZ12	Cell Signaling (3737)	WB (1:500) IP (5 µg) C&R 1:100
Rabbit anti-EZH2	Cell Signaling (5246)	WB 1:1000
Mouse anti-EED	MilliporeSigma (17-663)	WB (1:1000)
Rabbit anti-H3K27me3	Cell signaling (9733)	C&R 1:100
Rabbit anti-H2A.Z	Abcam (ab4174)	ChIP-seq (5 µg)
Mouse anti-alpha-Actin	Santa Cruz (sc-32251)	WB 1:2000
Mouse anti-SYCP3	Abcam (ab97672)	IF 1:1000

Supplementary Materials and Methods

Immunofluorescence staining

To make frozen blocks, testes were collected, cleaned and washed in Optimum Cutting Temperature (OCT) embedding medium before embedding in OCT. Alternatively, testes were collected, cleaned in PBS and fixed in 10% neutral buffered formalin at 4°C for 1 hour. Fixed tissues were washed in PBS for 3 times, 15 minutes each at 4˚C, followed by incubation once in 15% and twice in 30% sucrose respectively, for 1 hour each, on a nutator at 4˚C. Tissues were then washed with OCT for 10 minutes at RT followed by OCT embedding and storing at -80˚C.

Spermatocyte single cell spreads were prepared according to a previously described protocol (Wojtasz et al., 2009) with modifications (Biswas et al., 2018). Briefly, 2ul cell suspension was added to each slide containing 7µl 0.25% NP-40 and incubated for 2 minutes at RT. Fixative solution (24ul; 1% paraformaldehyde, 10 mM sodium borate buffer pH 9.2) was added to each slide and incubated in a moist chamber for 1 hour at RT. Slides were dried under a hood and washed in 0.5% Kodak Photo-flo 200 three times, 1 minute each, and stored at -80˚C.

Cryosections (7uM) were fixed in 10% freshly made paraformaldehyde solution in PBS for 10 minutes at 4˚C. Alternatively prefixed sections were washed in PBS 3 times, 5 minutes each, followed by antigen retrieval in boiling citrate buffer (10 mM citric acid, pH 6.0) for 10 min.

Tissue sections or cell spreads were washed and permeabilized in PBST (PBS + 0.1% Triton-X 100), 3 times for 5 minutes each, followed by blocking with blocking buffer

(10% goat/donkey serum, 2% bovine serum albumin, 0.01% Triton-X 100 in PBS) for 1 hour at RT before incubation with primary antibody (listed in Table. S5) in blocking buffer overnight at 4˚C. The next day, samples were washed 3 times, 5 minutes each with PBST and incubated with Alexa Fluor-conjugated secondary antibody for 1 hour at RT. Samples were washed 2 times, 5 minutes each with PBST and counterstained with DAPI. Slides were washed twice more in PBS before mounting in Prolong Gold anti-fade medium (P-36931; Life Technologies).

Nuclear lysate preparation

Spermatogenic cells isolated from CD1 males on P18 were resuspended in hypotonic buffer (buffer A:10mM HEPES-KOH pH7.9, 1.5mM $MgCl_2$, 10mM KCl, 0.1% NP-40, 5mM NaF, 1mM Na_3VO_4, 1mM PMSF, 1x Protease inhibitor cocktail) using 10-20 times the volume of the precipitated cell volume (PCV). The suspension was incubated on ice for 15 minutes and centrifuged at 1000g for 10 minutes at 4˚C. The precipitated cells were resuspended in 2 PCV of buffer A and homogenized using Dounce ‘B’ pestle 5 times in an ice-cold Dounce homogenizer, followed by centrifugation at 1000g for 10 minutes at 4˚C. Precipitated nuclei were washed in buffer A once more, followed by resuspension and incubation in equal volume lysis buffer (Buffer C) (20mM HEPES-KOH pH7.9, 1.5mM $MgCl_2$, 420mM NaCl, 10mM KCl, 25 % glycerol, 0.2mM EDTA, 5mM NaF, 1mM Na_3VO_4, 1mM PMSF, 1x Protease inhibitor cocktail) for 30 minutes at 4˚C on a nutator. The homogenate was centrifuged at 12000g for 10 minutes and the supernatant was transferred to a fresh centrifuge tube. The pellet was resuspended in an equal volume of Buffer C with 0.1% TritonX-100 and incubated for another 30 minutes at 4˚C on a nutator. The homogenate was centrifuged at 12000g for 10 minutes

and the supernatant collected and pooled together with the previous batch. Next, half of the total lysate was treated with 50µg/ml ethidium bromide and incubated on ice for 30 mins to inhibit DNA-protein interaction (Lai and Herr, 1992) followed by centrifugation at 12000g for 10 minutes. The supernatant was transferred to a fresh centrifuge tube followed by addition of 2.8 volume of dilution buffer (Buffer D) (20mM HEPES-KOH pH7.9, 20 % glycerol, 0.2mM EDTA, 5mM NaF, 1mM Na_3VO_4, 1mM PMSF, 1x Protease inhibitor cocktail) to all lysates. When necessary, DTT was added to the lysate at a final concentration of 1mM. These two batches of lysates were pooled together for co-immunoprecipitation.

Co-Immunoprecipitation

Protein A conjugated Dynabeads (Invitrogen) (50ul per sample) were washed in PBS and incubated in PBS + 0.5% BSA for 10 minutes. Further, the beads were washed once in PBS, and twice in immunoprecipitation (IP) buffer (20mM HEPES-KOH pH7.9, 0.15mM KCl, 10% glycerol, 0.2mM EDTA, 0.5mM PMSF, 1x Protease inhibitor cocktail). 1-1.5 mg nuclear lysate were diluted with IP buffer to reach a concentration of 1mg/ml and precleared with prepared protein A conjugated Dynabeads on a nutator at 4˚C for 30 minutes. Following the removal of the Dynabeads, primary antibody (listed in Table. S5) was added, and the sample was incubated on a nutator at 4˚C for 30 minutes. At this point, prepared magnetic beads were added to each sample and incubated overnight at 4˚C on a nutator. The next day, each sample was washed 2X in IP wash buffer (20mM HEPES-KOH pH7.9, 0.15mM KCl, 10% glycerol, 0.2mM EDTA, 1mM PMSF, 1x Protease inhibitor cocktail), 1X in high salt wash buffer (20mM HEPES-KOH pH7.9, 300mM KCl, 10 % glycerol, 0.2mM EDTA, 0.1 % Tween-20, 1mM PMSF, 1x

Protease inhibitor cocktail) and 1X in low salt wash buffer (20mM HEPES-KOH pH7.9, 100mM KCl, 10 % glycerol, 0.2mM EDTA, 0.1 % Tween-20, 1mM PMSF, 1x Protease inhibitor cocktail). The samples were then washed once in final wash buffer (20mM HEPES-KOH pH7.9, 60mM KCl, 10 % glycerol, 1mM PMSF, 1x Protease inhibitor cocktail). Proteins were eluted by adding 1.3X Laemmli buffer and incubating at 65˚C for 15 minutes, followed by removal of Dynabeads and heating the samples at 95˚C for 5 minutes.

Data analysis

RNAseq reads were aligned using Tophat2 (Kim et al., 2013) and the aligned reads counted by HTseqCount (Anders et al., 2015). Differential expression analysis was done by using DESeq2 (Love et al., 2014) with recommended settings (Table. S2). Volcano plots were generated using the EnhancedVolcano package (https://github.com/kevinblighe/EnhancedVolcano). Pathway enrichment analyses were done using ClusterProfiler (Yu et al., 2012) and Gene Set Enrichment Analyses (Subramanian et al., 2005). Anatomical relevance to the gene sets were determined by EMAPA signature using the Mousemine.org website.

ChIP-seq data were analyzed by trimming the reads as necessary using trimmomatic (Bolger et al., 2014) and aligning reads to the reference genome mm10 using Bowtie2 (Langmead and Salzberg, 2012) with sensitive settings. Alignments were de-duplicated and replicates merged using Samtools (Danecek et al., 2021; Li et al., 2009). Coverage tracks (BigWig files) were created using Deeptools (Ramírez et al., 2016), extending fragments to 150bp, filtering for mm10 backlisted regions, and with RPKM normalization based on the reads from autosomes. Bigwig files were visualized using the UCSC

genome browser (Kent et al., 2002). Metaplots and heatmaps were created using Deeptools (Ramírez et al., 2016). Peaks were called by MACS2 (Zhang et al., 2008) using the options –extsize set to 147 and –nomodel (Table. S1 and S3). Peak annotation was performed by annotatePeak.pl in Homer (Heinz et al., 2010). Differential binding analysis was performed by CSAW (Lun and Smyth, 2015) using region-based binned read count followed by TMM normalization using genome-wide background estimation. Plots were created in R using ggplot2 (Wickham, 2016).

CUT&RUN reads were aligned to the reference genome mm10 using Bowtie2 (Langmead and Salzberg, 2012) with very-sensitive setting allowing dovetail alignment. Duplicates were marked by Picard (https://broadinstitute.github.io/picard/) and replicates were merged using Samtools (Danecek et al., 2021; Li et al., 2009). Coverage tracks were prepared from merged files with 1X normalization based on the reads from autosomes using Deeptools (Ramírez et al., 2016), extending fragments to 150bp and filtering for mm10 blacklisted regions. Metaplots were created using Deeptools (Ramírez et al., 2016). Differential binding analysis was performed by CSAW (Lun and Smyth, 2015) using region-based binned read count followed by TMM normalization using genome-wide background estimation. Plots were created in R using ggplot2 (Wickham, 2016).

ATAC-seq reads were processed using nf-core/atacseq (ver 1.1.0) pipeline (Ewels et al., 2020). In short, the reads were trimmed using Trim Galore (https://www.bioinformatics.babraham.ac.uk/projects/trim_galore/) and aligned to mm10 using BWA. Duplicates were marked by Picard (https://broadinstitute.github.io/picard/). Normalized coverage tracks (BigWig files) were created from merged replicates scaled

to 1 million mapped reads using BEDTools and read coverage over regions of interest were created using Deeptools (Ramírez et al., 2016). Differential accessibility analysis was performed by CSAW (Lun and Smyth, 2015) using region-based binned read count followed by TMM normalization using genome-wide background estimation. Plots were created in R using ggplot2 (Wickham, 2016).

References

Anders, S., Pyl, P. T. and Huber, W. (2015). HTSeq-A Python framework to work with high-throughput sequencing data. *Bioinformatics* **31**, 166–169.

Biswas, U., Stevense, M. and Jessberger, R. (2018). SMC1α Substitutes for Many Meiotic Functions of SMC1β but Cannot Protect Telomeres from Damage. *Curr. Biol.* **28**, 249-261.e4.

Bolger, A. M., Lohse, M. and Usadel, B. (2014). Trimmomatic: A flexible trimmer for Illumina sequence data. *Bioinformatics* **30**, 2114–2120.

Danecek, P., Bonfield, J. K., Liddle, J., Marshall, J., Ohan, V., Pollard, M. O., Whitwham, A., Keane, T., McCarthy, S. A., Davies, R. M., et al. (2021). Twelve years of SAMtools and BCFtools. *Gigascience* **10**, 1–4.

Ewels, P. A., Peltzer, A., Fillinger, S., Patel, H., Alneberg, J., Wilm, A., Garcia, M. U., Di Tommaso, P. and Nahnsen, S. (2020). The nf-core framework for community-curated bioinformatics pipelines. *Nat. Biotechnol.* **38**, 276–278.

Heinz, S., Benner, C., Spann, N., Bertolino, E., Lin, Y. C., Laslo, P., Cheng, J. X., Murre, C., Singh, H. and Glass, C. K. (2010). Simple Combinations of Lineage-Determining Transcription Factors Prime cis-Regulatory Elements Required for Macrophage and B Cell Identities. *Mol. Cell* **38**, 576–589.

Kent, W. J., Sugnet, C. W., Furey, T. S., Roskin, K. M., Pringle, T. H., Zahler, A. M. and Haussler, a. D. (2002). The Human Genome Browser at UCSC. *Genome Res.* **12**, 996–1006.

Kim, D., Pertea, G., Trapnell, C., Pimentel, H., Kelley, R. and Salzberg, S. L. (2013). TopHat2: Accurate alignment of transcriptomes in the presence of insertions, deletions and gene fusions. *Genome Biol.* **14**, R36.

Lai, J. S. and Herr, W. (1992). Ethidium bromide provides a simple tool for identifying genuine DNA- independent protein associations. *Proc. Natl. Acad. Sci. U. S. A.* **89**, 6958–6962.

Langmead, B. and Salzberg, S. L. (2012). Fast gapped-read alignment with Bowtie 2. *Nat. Methods* **9**, 357–359.

Li, H., Handsaker, B., Wysoker, A., Fennell, T., Ruan, J., Homer, N., Marth, G., Abecasis, G. and Durbin, R. (2009). The Sequence Alignment/Map format and SAMtools. *Bioinformatics* **25**, 2078–2079.

Love, M. I., Huber, W. and Anders, S. (2014). Moderated estimation of fold change and dispersion for RNA-seq data with DESeq2. *Genome Biol.* **15**, 550.

Lun, A. T. L. and Smyth, G. K. (2015). Csaw: A Bioconductor package for differential binding analysis of ChIP-seq data using sliding windows. *Nucleic Acids Res.* **44**, e45.

Ramírez, F., Ryan, D. P., Grüning, B., Bhardwaj, V., Kilpert, F., Richter, A. S., Heyne, S., Dündar, F. and Manke, T. (2016). deepTools2: a next generation web server for deep-sequencing data analysis. *Nucleic Acids Res.* **44**, 160–165.

Subramanian, A., Tamayo, P., Mootha, V. K., Mukherjee, S., Ebert, B. L., Gillette, M. A., Paulovich, A., Pomeroy, S. L., Golub, T. R., Lander, E. S., et al. (2005). Gene set enrichment analysis: A knowledge-based approach for interpreting genome-wide expression profiles. *Proc. Natl. Acad. Sci. U. S. A.* **102**, 15545–15550.

Wickham, H. (2016). *ggplot2: Elegant Graphics for Data Analysis*. Springer-Verlag New York.

Wojtasz, L., Daniel, K., Roig, I., Bolcun-Filas, E., Xu, H., Boonsanay, V., Eckmann, C. R., Cooke, H. J., Jasin, M., Keeney, S., et al. (2009). Mouse HORMAD1 and HORMAD2, two conserved meiotic chromosomal proteins, are depleted from synapsed chromosome axes with the help of TRIP13 AAA-ATPase. *PLoS Genet.* **5**, e1000702.

Yu, G., Wang, L. G., Han, Y. and He, Q. Y. (2012). ClusterProfiler: An R package for comparing biological themes among gene clusters. *Omi. A J. Integr. Biol.* **16**, 284–287.

Zhang, Y., Liu, T., Meyer, C. A., Eeckhoute, J., Johnson, D. S., Bernstein, B. E., Nussbaum, C., Myers, R. M., Brown, M., Li, W., et al. (2008). Model-based analysis of ChIP-Seq (MACS). *Genome Biol.* **9**, R137.